Fibonacci and Lucas Points and Their Inverse Stereographic Projections onto Deformed Spheres

BARIS ATES
Department of Mathematics Piri Reis University
Postane, Eflatun Sk. No:8, 34940 Tuzla
TÜRKIYE

Abstract: Fibonacci and Lucas numbers play a distinguished role in mathematics, science, and nature, while their generalized forms arise in a wide variety of scientific applications. Point sets generated from these special sequences provide highly structured distributions on the Euclidean plane and can be transferred onto spherical surfaces through inverse stereographic projection. In this work, we extend this framework by considering inverse stereographic projections onto deformed spheres obtained through arbitrary single-valued surface deformation functions. This construction enables the generation of special point distributions on infinitely many classes of surfaces, including rotationally symmetric and non-symmetric geometries, as well as differentiable and non-differentiable surfaces. A fundamental result of the study is that the projected Fibonacci and Lucas points are not distributed arbitrarily on these deformed surfaces. Instead, their coordinates satisfy recurrence relations whose forms explicitly depend on the surface deformation functions. Consequently, the algebraic structure inherited from Fibonacci and Lucas sequences becomes intrinsically linked to the geometry of the underlying surface. This establishes a direct connection between discrete number-theoretic sequences and continuous surface deformations. Since the deformation functions are arbitrary, the obtained results remain valid for an infinite family of geometries, providing a versatile framework for studying structured point distributions on non-spherical surfaces. The proposed approach opens a new avenue connecting abstract number theory with surface theory and offers potential applications in geometry, mathematical physics, computational modeling, and the analysis of naturally occurring shapes.

Key-Words: Fibonacci Numbers · Lucas Numbers · Stereographic Projection · Deformed Spheres

Received: March 11, 2026. Revised: June 13, 2026. Accepted: July 15, 2026. Available online: November 25, 2026.

1 Introduction

The Fibonacci and Lucas sequences are the two important series of the number theory that shares the same recurrence relation

$$\Psi_{n+2} = \Psi_n + \Psi_{n+1}. \tag{1}$$

If the initial numbers are $\Psi_0 = 0$ and $\Psi_1 = 1$, then this sequence is the Fibonacci sequence, $\Psi_n = F_n$. Similarly if the initial numbers $\Psi_0 = 2$ and $\Psi_1 = 1$, then this sequence is the Lucas sequence, $\Psi_n = L_n$. This shared structure leads to a rich web of identities and asymptotic properties, many of which are governed by the golden ratio. Beyond their algebraic elegance, these sequences manifest in a wide spectrum of natural phenomena. Spiral arrangements in plants, branching patterns, and growth processes frequently reflect Fibonacci type order, while Lucas numbers, though less commonly emphasized, arise naturally in combinatorial interpretations and in the study of periodic structures. The significance of these sequences extends well beyond classical examples. In modern scientific contexts, Fibonacci and Lucas configurations appear in areas such as quasicrystals, wave interference patterns, and information encoding schemes. Their recursive nature provides a bridge between discrete models and continuous behavior, allowing them to serve as a foundation for constructing structured point distributions [1, 2, 3, 4, 5, 6, 7]. When viewed through this lens, both sequences can be treated as generators of geometric configurations, rather than merely numerical objects. A natural question, therefore, is how such discrete structures behave when transported from flat spaces to curved geometries. One of the most powerful mechanisms for achieving this transition is inverse stereographic projection. As the inverse of a classical conformal map, it establishes a correspondence between the Euclidean plane and the unit sphere, preserving angular relationships while redistributing distances in a non-uniform manner [8, 9]. This transformation is particularly well suited for discrete sets defined by algebraic rules, since it maps sequences of planar points into structured distributions on curved surfaces without destroying their intrinsic order [10]. When Fibonacci or Lucas based point sets are subjected to this mapping, their

geometric interpretation changes in a subtle but meaningful way. Linear alignments in the plane may transform into curved arrangements on the sphere, and algebraic identities can acquire geometric counterparts involving spherical distances or angular separations. Because both sequences share the same recurrence, their induced configurations often exhibit parallel behaviors, yet important differences emerge due to their distinct initial conditions. This duality provides an additional layer of structure that can be exploited in geometric analysis. The framework becomes even more flexible when the target surface is allowed to deviate from perfect spherical symmetry. By introducing controlled deformations along the normal direction, through single valued scalar functions, one obtains a broad class of surfaces ranging from spheroids to more irregular shapes [11, 12, 13]. Despite these deformations, the bijective relationship with the plane can often be preserved, ensuring that the essential features of the original point sets remain accessible. This opens the door to modeling geometric patterns on surfaces that more closely resemble those encountered in nature, where ideal symmetry is rarely observed. In this study, we develop a systematic approach to transferring Fibonacci and Lucas configurations from the Euclidean plane to spherical and deformed spherical geometries in arbitrary D dimensional space. Beginning with planar point sets defined via these sequences, we apply inverse stereographic projection to obtain their images on S^2, and we analyze how classical identities manifest in this new setting [10, 14]. We then extend the construction by incorporating analytic surface deformations, thereby generating families of geometries on which these number theoretic structures can be realized [11, 12]. Through this perspective, Fibonacci and Lucas sequences are reinterpreted as tools for encoding geometric information on curved surfaces, with potential implications for both theoretical investigations and applications in natural and physical systems.

2 Inverse Stereographic Projection of Fibonacci and Lucas Points

The Fibonacci points on the plane are the points such that, the absolute value of each coordinate of the point is a Fibonacci number [10]. A similar definition can be followed to reach the Lucas points on the plane. Thus their mathematical expressions are in the following form:

$$P^F(x,y) = P^F(c_1F_n, c_2F_m) \tag{2}$$
$$P^L(x,y) = P^L(c_1L_n, c_2L_m) \tag{3}$$

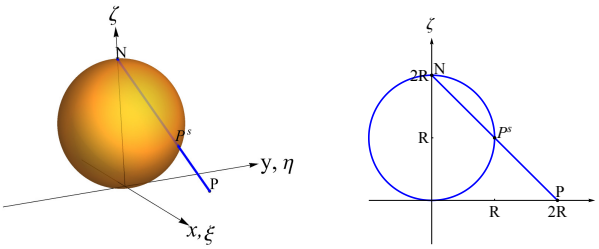

Figure 1: Stereographic projection of a point on the sphere $p^s(\xi,\eta,\zeta)$ to the plane point $P(x,y)$, and 2D view of the set up.

where c_1 and c_2 are either $+1$ or -1. Stereographic projection is an one to one mapping (Except for the north point N) that relates points on the plane with the ones on the sphere. Let us assume that, the center of the sphere is located at the ζ axis $(0,0,R)$. Thus, its mathematical expression is given as $\xi^2+\eta^2+(\zeta-R)^2=R^2$. It is well known that a point on the sphere $P(\xi,\eta,\zeta)$ is mapped to a unique point $P(x,y)$ on the $x-y$ plane via stereographic projection as shown in Fig. 1. The mathematical expression of this relation is given by following relation

$$\xi = \frac{4R^2x}{4R^2+x^2+y^2}$$
$$\eta = \frac{4R^2y}{4R^2+x^2+y^2}$$
$$\zeta = \frac{2R(x^2+y^2)}{4R^2+x^2+y^2}$$

and conversely, the inverse stereographic projection of a point $P(x,y)$ is found by the following relation[8], [9]:

$$P(x,y) = P\left(\frac{2R\xi}{2R-\zeta}, \frac{2R\eta}{2R-\zeta}\right). \tag{4}$$

The ISP of a Fibonacci and Lucas point is given by the following relation:

$$\xi^{\Psi}_{n,m} = \frac{4R^2c_1\Psi_n}{4R^2+\Psi_n^2+\Psi_m^2}$$
$$\eta^{\Psi}_{n,m} = \frac{4R^2c_2\Psi_m}{4R^2+\Psi_n^2+\Psi_m^2}$$
$$\zeta^{\Psi}_{n,m} = \frac{2R(\Psi_n^2+\Psi_m^2)}{4R^2+\Psi_n^2+\Psi_m^2} \tag{5}$$

Let us consider special Fibonacci and Lucas points $P_n(\Psi_n,0)$ on the x-axis, whose first coordinates are Fibonacci or Lucas numbers, i.e., If Ψ_n is

chosen as $\Psi_n = F_n$, these points are the Fibonacci points; $P_0(0,0), P_1(1,0), P_2(1,0), P_3(2,0), \ldots,$ $P_n(F_n,0)$ and if Ψ_n is chosen as $\Psi_n = L_n$, these points are the Lucas points; $P_0(2,0), P_1(1,0), P_2(3,0), \ldots, P_n(L_n,0)$. The coordinates of the image points $P\left(\xi_n^\Psi, \eta_n^\Psi, \zeta_n^\Psi\right)$, under the inverse stereographic projection of $P_n(\Psi_n,0)$, are obtained as

$$P\left(\xi_n^\Psi, \eta_n^\Psi, \zeta_n^\Psi\right) = P\left(\frac{4R^2\Psi_n}{4R^2+\Psi_n^2}, 0, \frac{2R\Psi_n^2}{4R^2+\Psi_n^2}\right).$$

In order to find a relation for the ξ_n^Ψ, one can consider the first coordinates and rearrange them as $\xi_n^\Psi \Psi_n^2 - 4R^2\Psi_n + 4R^2\xi_n^\Psi = 0$ which yields

$$\Psi_n = \frac{2R^2 + 2R\lambda_n\sqrt{R^2-(\xi_n^\Psi)^2}}{\xi_n^\Psi},\ \xi_n^\Psi \neq 0 \quad (6)$$

where $\xi_n^\Psi \neq 0$ and $\lambda_n = \lambda_n(R) \in \{-1,+1\}$ is the sign that selects the appropriate root of the quadratic equation above [10] . The condition $\xi_n^\Psi \neq 0$ excludes only the Fibonacci point $P_0(0,0)$ ($F_0 = 0$), whose image is the origin $(0,0,0)$; it is always satisfied for Lucas points. For a given ξ_n^Ψ, the two roots of the quadratic equation are Ψ_n and $4R^2/\Psi_n$, since their product is $4R^2$. Hence the smaller root ($\Psi_n < 2R$) corresponds to $\lambda_n = -1$ and the larger root ($\Psi_n > 2R$) to $\lambda_n = +1$, that is,

$$\lambda_n(R) = \begin{cases} -1, & \Psi_n < 2R, \\ +1, & \Psi_n > 2R. \end{cases} \quad (7)$$

When $\Psi_n = 2R$, we have $\xi_n^\Psi = R$, the square root in (6) vanishes, and the value of λ_n is immaterial. Thus, one can conclude that the coordinates of the ISP of the sequential points $P_n(\Psi_n,0)$ satisfy the following nonlinear addition relations:

$$\frac{2R^2 + 2\lambda_n R\sqrt{R^2-(\xi_n^\Psi)^2}}{\xi_n^\Psi} + \frac{2R^2 + 2\lambda_{n+1} R\sqrt{R^2-(\xi_{n+1}^\Psi)^2}}{\xi_{n+1}^\Psi} = \frac{2R^2 + 2\lambda_{n+2} R\sqrt{R^2-(\xi_{n+2}^\Psi)^2}}{\xi_{n+2}^\Psi}, \quad (8)$$

$$\eta_n^\Psi = \eta_{n+1}^\Psi = \eta_{n+2}^\Psi = 0, \quad (9)$$

$$\sqrt{\frac{\zeta_n^\Psi}{2R-\zeta_n^\Psi}} + \sqrt{\frac{\zeta_{n+1}^\Psi}{2R-\zeta_{n+1}^\Psi}} = \sqrt{\frac{\zeta_{n+2}^\Psi}{2R-\zeta_{n+2}^\Psi}}, \quad (10)$$

$$\frac{2R\,\xi_n^\Psi}{2R-\zeta_n^\Psi} + \frac{2R\,\xi_{n+1}^\Psi}{2R-\zeta_{n+1}^\Psi} = \frac{2R\,\xi_{n+2}^\Psi}{2R-\zeta_{n+2}^\Psi} \quad (11)$$

where short hand notation $\lambda_n = \lambda_n(R)$ is used and they are equal to ± 1 for any n.

2.1 Rotation of Fibonacci and Lucas Points

The rotation of the special Fibonacci and Lucas points $P_n(\Psi_n,0)$ about the origin by an angle according to the transformation rule

$$\begin{aligned} x^{\text{rot}} &= \cos\alpha\ x - \sin\alpha\ y \\ y^{\text{rot}} &= \sin\alpha\ x + \cos\alpha\ y \end{aligned} \quad (12)$$

allows one to obtain new points $P^{\text{rot}}(x^{\text{rot}}, y^{\text{rot}})$ such that their distance to the origin is a Fibonacci or Lucas number [10]. ISP of those rotated Fibonacci and Lucas points also satisfy following nonlinear addition relations:

$$\frac{2R^2\cos\alpha + 2\lambda_n^{\text{rot}} R\sqrt{R^2\cos^2\alpha-(\xi_n^{\text{rot}})^2}}{\xi_n^{\text{rot}}} + \frac{2R^2\cos\alpha + 2\lambda_{n+1}^{\text{rot}} R\sqrt{R^2\cos^2\alpha-(\xi_{n+1}^{\text{rot}})^2}}{\xi_{n+1}^{\text{rot}}} = \frac{2R^2\cos\alpha + 2\lambda_{n+2}^{\text{rot}} R\sqrt{R^2\cos^2\alpha-(\xi_{n+2}^{\text{rot}})^2}}{\xi_{n+2}^{\text{rot}}}, \quad (13)$$

$$\frac{2R^2\sin\alpha + 2\lambda_n^{\text{rot}} R\sqrt{R^2\sin^2\alpha-(\eta_n^{\text{rot}})^2}}{\eta_n^{\text{rot}}} + \frac{2R^2\sin\alpha + 2\lambda_{n+1}^{\text{rot}} R\sqrt{R^2\sin^2\alpha-(\eta_{n+1}^{\text{rot}})^2}}{\eta_{n+1}^{\text{rot}}} = \frac{2R^2\sin\alpha + 2\lambda_{n+2}^{\text{rot}} R\sqrt{R^2\sin^2\alpha-(\eta_{n+2}^{\text{rot}})^2}}{\eta_{n+2}^{\text{rot}}}, \quad (14)$$

$$\sqrt{\frac{\zeta_n^{\text{rot}}}{2R-\zeta_n^{\text{rot}}}} + \sqrt{\frac{\zeta_{n+1}^{\text{rot}}}{2R-\zeta_{n+1}^{\text{rot}}}} = \sqrt{\frac{\zeta_{n+2}^{\text{rot}}}{2R-\zeta_{n+2}^{\text{rot}}}} \quad (15)$$

where λ_n^{rot}s are equal to ± 1 [10]. Their exact values depend on R, n, and α. In (13) and (14), additional $\cos\alpha$ and $\sin\alpha$ terms appear, respectively. Hence in (13) and (14), $\lambda_n^{\text{rot}} = \text{sgn}(\cos\alpha)\,\lambda_n$ and $\lambda_n^{\text{rot}} = \text{sgn}(\sin\alpha)\,\lambda_n$, respectively. The cases $\cos\alpha = 0$ and $\sin\alpha = 0$ are trivial, since the corresponding component of every image point vanishes.

The relations between the mixed coordinates of the images of the points on the rotated line can also be

obtained from the Equation (4) as

$$\frac{\xi_n^{\text{rot}}}{2R-\zeta_n^{\text{rot}}}+\frac{\xi_{n+1}^{\text{rot}}}{2R-\zeta_{n+1}^{\text{rot}}}=\frac{\xi_{n+2}^{\text{rot}}}{2R-\zeta_{n+2}^{\text{rot}}} \quad (16)$$

$$\frac{\eta_n^{\text{rot}}}{2R-\zeta_n^{\text{rot}}}+\frac{\eta_{n+1}^{\text{rot}}}{2R-\zeta_{n+1}^{\text{rot}}}=\frac{\eta_{n+2}^{\text{rot}}}{2R-\zeta_{n+2}^{\text{rot}}}. \quad (17)$$

After finding identities for the special Fibonacci and Lucas points, one can proceed to the most general Lucas and Fibonacci points $P\left(c_1\Psi_n, c_2\Psi_m\right)$. In this case, inverse stereographic projection allows to find the following relations between the coordinates of the sequential points:

$$\frac{\xi_{n,m}}{2R-\zeta_{n,m}}+\frac{\xi_{n+1,m}}{2R-\zeta_{n+1,m}}=\frac{\xi_{n+2,m}}{2R-\zeta_{n+2,m}} \quad (18)$$

$$\frac{\eta_{n,m}}{2R-\zeta_{n,m}}+\frac{\eta_{n,m+1}}{2R-\zeta_{n,m+1}}=\frac{\eta_{n,m+2}}{2R-\zeta_{n,m+2}}. \quad (19)$$

2.2 Inverse Stereographic Projection of Fibonacci and Lucas Points onto the Deformed Spheres

The mapping between points on the sphere and those on the plane established through stereographic projection can also be extended to spheres that are deformed [11, 12]. A point on a sphere centered at the origin has the position vector expressed in spherical coordinates as $\vec{r}_{\text{sph}} = R\,\hat{r}$. A radial deformation of this sphere can be introduced via the relation [12]

$$\vec{r}_{\text{d}} = R(1+\beta f(\theta,\varphi))\,\hat{r} \quad (20)$$

where $f(\theta,\varphi)$ denotes an arbitrary single-valued function and β represents the deformation parameter. To determine the images of planar points on such deformed spheres using ISP, one can begin by mapping the point $P^{(0)}\,(x\,,y)$ onto the sphere through (5), yielding the point $P^{(1)} = (\xi^{(1)},\eta^{(1)},\zeta^{(1)})$. Since this sphere is centered along the ζ-axis, applying a translation leads to a new point $P^{(2)} = (\xi^{(2)},\eta^{(2)},\zeta^{(2)}) = \left(\xi^{(1)},\eta^{(1)},\zeta^{(1)}-R\right)$ on a sphere whose center is at the origin. Since the deformation function is expressed in terms of the angular variables θ and φ, the radial displacement varies depending on the location of the point on the sphere. Therefore, to utilize (20), which describes the surface deformation, it is necessary to determine these spherical angles. The angles θ and φ can be obtained using the following relations:

$$\theta = \arccos\left(\frac{\zeta^{(2)}}{R}\right), \qquad \varphi = arctan2(\eta^{(2)},\xi^{(2)}). \quad (21)$$

Once the spherical angles are found, according to the deformation (20), one can obtain a new point $P^{(3)} = (\xi^{(3)},\eta^{(3)},\zeta^{(3)})$ on deformed sphere with the following relations:

$$\xi^{(3)} = \xi^{(2)} + \beta R f\left(\theta,\varphi\right)\sin\left(\theta\right)\cos\left(\varphi\right) \quad (22)$$

$$\eta^{(3)} = \eta^{(2)} + \beta R f\left(\theta,\varphi\right)\sin\left(\theta\right)\sin\left(\varphi\right) \quad (23)$$

$$\zeta^{(3)} = \zeta^{(2)} + \beta R f\left(\theta,\varphi\right)\cos\left(\theta\right). \quad (24)$$

The final point $P^{(3)}$ is the inverse stereographic projection of $P^{(0)}$ onto the deformed sphere. For the uniqueness of the transformation one may consult [12].

In order to discuss the ISP of the Fibonacci and Lucas points onto the deformed spheres, let us consider special Fibonacci and Lucas points on the x axis. Since they are in the form of $P(\Psi_n,0)$. The image points on the deformed spheres that are obtained according to the relation (20) satisfy Fibonacci and Lucas recurrence relation as:

$$\frac{2R^2+2\lambda_n R\sqrt{R^2-(\xi_n^{(3)}-\beta f_n R\sin\theta_n\cos\varphi_n)^2}}{\xi_n^{(3)}-\beta f_n R\sin\theta_n\cos\varphi_n} + \frac{2R^2+2\lambda_{n+1} R\sqrt{R^2-(\xi_{n+1}^{(3)}-\beta f_{n+1} R\sin\theta_{n+1}\cos\varphi_{n+1})^2}}{\xi_{n+1}^{(3)}-\beta f_{n+1} R\sin\theta_{n+1}\cos\varphi_{n+1}} = \frac{2R^2+2\lambda_{n+2} R\sqrt{R^2-(\xi_{n+2}^{(3)}-\beta f_{n+2} R\sin\theta_{n+2}\cos\varphi_{n+2})^2}}{\xi_{n+2}^{(3)}-\beta f_{n+2} R\sin\theta_{n+2}\cos\varphi_{n+2}} \quad (25)$$

when the denominators are non zero. Since $\Psi_n = 2R$ corresponds to $\zeta_n^{(2)} = 0$, this can be written as $\lambda_n = \text{sgn}(\cos\theta_n)$, with θ_n given by (21). The factors $\xi_n^{(3)} - \beta f_n R\sin\theta_n\cos\varphi_n$ and $\eta_n^{(3)} - \beta f_n R\sin\theta_n\sin\varphi_n$ equal the undeformed coordinates $\xi_n^{(2)}$ and $\eta_n^{(2)}$, so the deformation does not change the branch signs.

Let us consider rotation of the special Fibonacci and Lucas Points $(\Psi_n,0)$ with an angle α according to the relation (12). After evaluating the ISP of these rotated points onto the deformed sphere, then it can be shown that, ξ components of the image points satisfy following recurrence relation;

$$\frac{2R^2\cos\alpha+2\lambda_n^{\text{rot}} R\sqrt{R^2\cos^2\alpha-(\xi_n^{(3)}-\beta f_n R\sin\theta_n\cos\varphi_n)^2}}{\xi_n^{(3)}-\beta f_n R\sin\theta_n\cos\varphi_n} + \frac{2R^2\cos\alpha+2\lambda_{n+1}^{\text{rot}} R\sqrt{R^2\cos^2\alpha-(\xi_{n+1}^{(3)}-\beta f_{n+1} R\sin\theta_{n+1}\cos\varphi_{n+1})^2}}{\xi_{n+1}^{(3)}-\beta f_{n+1} R\sin\theta_{n+1}\cos\varphi_{n+1}} = \frac{2R^2\cos\alpha+2\lambda_{n+2}^{\text{rot}} R\sqrt{R^2\cos^2\alpha-(\xi_{n+2}^{(3)}-\beta f_{n+2} R\sin\theta_{n+2}\cos\varphi_{n+2})^2}}{\xi_{n+2}^{(3)}-\beta f_{n+2} R\sin\theta_{n+2}\cos\varphi_{n+2}} \quad (26)$$

The η components of the image points satisfy

following relation

$$\frac{2R^2\sin\alpha+2\lambda_n^{\text{rot}}R\sqrt{R^2\sin^2\alpha-(\eta_n^{(3)}-\beta f_nR\sin\theta_n\sin\varphi_n)^2}}{\eta_n^{(3)}-\beta f_nR\sin\theta_n sin\varphi_n}$$
$$+\frac{2R^2\sin\alpha+2\lambda_{n+1}^{\text{rot}}R\sqrt{R^2\sin^2\alpha-(\eta_{n+1}^{(3)}-\beta f_{n+1}R\sin\theta_{n+1}\sin\varphi_{n+1})^2}}{\eta_{n+1}^{(3)}-\beta f_{n+1}R\sin\theta_{n+1}\sin\varphi_{n+1}}$$
$$=\frac{2R^2\sin\alpha+2\lambda_{n+2}^{\text{rot}}R\sqrt{R^2\sin^2\alpha-(\eta_{n+2}^{(3)}-\beta f_{n+2}R\sin\theta_{n+2}\sin\varphi_{n+2})^2}}{\eta_{n+2}^{(3)}-\beta f_{n+2}R\sin\theta_{n+2}\sin\varphi_{n+2}} \tag{27}$$

and finally the ζ components satisfy the recurrence relation:

$$\sqrt{\frac{\zeta_n^{(3)}+R(1-\beta f_n\cos\theta_n)}{R(1+\beta f_n\cos\theta_n)-\zeta_n^{(3)}}}+\sqrt{\frac{\zeta_{n+1}^{(3)}+R(1-\beta f_{n+1}\cos\theta_{n+1})}{R(1+\beta f_{n+1}\cos\theta_{n+1})-\zeta_{n+1}^{(3)}}}$$
$$=\sqrt{\frac{\zeta_{n+2}^{(3)}+R(1-\beta f_{n+2}\cos\theta_{n+2})}{R(1+\beta f_{n+2}\cos\theta_{n+2})-\zeta_{n+2}^{(3)}}}. \tag{28}$$

The last equation does not explicitly depends on the α, in fact α dependency implicitly exist in φ_n and f_n.

After considering special Fibonacci and Lucas points, let us consider the most general Fibonacci and Lucas points $P=(c_1\Psi_n, c_2\Psi_m)$. ISP of those points on the deformed spheres satisfy following identities [11]:

$$\frac{\xi_{n,m}^{(3)}-R\beta f_{n,m}\sin\theta_{n,m}\cos\varphi_{n,m}}{R(1+\beta f_{n,m}\cos\theta_{n,m})-\zeta_{n,m}^{(3)}}$$
$$+\frac{\xi_{n+1,m}^{(3)}-R\beta f_{n+1,m}\sin\theta_{n+1,m}\cos\varphi_{n+1,m}}{R(1+\beta f_{n+1,m}\cos\theta_{n+1,m})-\zeta_{n+1,m}^{(3)}}$$
$$=\frac{\xi_{n+2,m}^{(3)}-R\beta f_{n+2,m}\sin\theta_{n+2,m}\cos\varphi_{n+2,m}}{R(1+\beta f_{n+2,m}\cos\theta_{n+2,m})-\zeta_{n+2,m}^{(3)}} \tag{29}$$

and

$$\frac{\eta_{n,m}^{(3)}-R\beta f_{n,m}\sin\theta_{n,m}\sin\varphi_{n,m}}{R(1+\beta f_{n,m}\cos\theta_{n,m})-\zeta_{n,m}^{(3)}}$$
$$+\frac{\eta_{n,m+1}^{(3)}-R\beta f_{n,m+1}\sin\theta_{n,m+1}\sin\varphi_{n,m+1}}{R(1+\beta f_{n,m+1}\cos\theta_{n,m+1})-\zeta_{n,m+1}^{(3)}}$$
$$=\frac{\eta_{n,m+2}^{(3)}-R\beta f_{n,m+2}\sin\theta_{n,m+2}\sin\varphi_{n,m+2}}{R(1+\beta f_{n,m+2}\cos\theta_{n,m+2})-\zeta_{n,m+2}^{(3)}}. \tag{30}$$

These two equations, together with the (20), allows one to find $\xi_{n+2}^{(3)}, \eta_{n+2}^{(3)}, \zeta_{n+2}^{(3)}$ when $\xi_n^{(3)}, \eta_n^{(3)}, \zeta_n^{(3)}$ and $\xi_{n+1}^{(3)}, \eta_{n+1}^{(3)}, \zeta_{n+1}^{(3)}$ are known. The general Fibonacci numbers $P_{n,m}(c_1F_n, c_2F_m)$ has quite interesting properties. For the fixed m, if one considers the sequential points $P_{n,m}$, $P_{n+1,m}$, and $P_{n+2,m}$ which are the points located on the line $y=c_2F_m$, then ISP of those points satisfy the relation (29), likewise, for the fixed n, if one considers the sequential points $P_{n,m}$, $P_{n,m+1}$, and $P_{n,m+2}$ which are the points located on the line $x=c_1F_n$, then ISP of those points satisfy the relation (30).

To illustrate the above procedure, let us consider a special griding of the plane with the Fibonacci related lines $x=\pm F_n$ and $y=\pm F_m$. In this grid the intersection of the gridlines are the Fibonacci points (c_1F_n, c_2F_m). This grid is shown in Fig. 2a. ISP of this grid divides the surface of the sphere in terms of Fibonacci related curves as shown in Fig. 2b. It should be noted that, intersection of those curves are ISP of the Fibonacci points. In Fig. 2c. ISP of the grid onto the deformed sphere is shown. For this case deformed sphere is obtained for the choice of parameters, $R=1$, $\beta=0.3$ and $f(\theta,\varphi)=\text{Re}(Y_7^2(\theta,\varphi))$ where $Y_n^m(\theta,\varphi)$ denotes spherical harmonics and Re(.) denotes the real part of its argument.

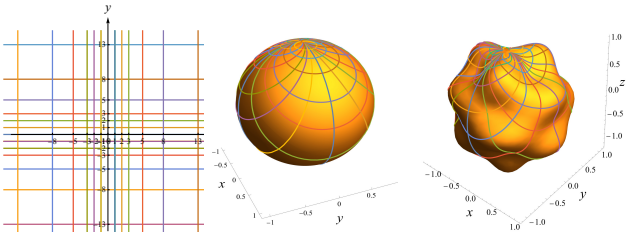

(a) (b) (c)

Figure 2: (a) Fibonacci grids on the plane. (b) ISP of the grid lines onto the sphere (c) ISP of the grid lines onto the deformed sphere .

3 Fibonacci and Lucas Identities and Their Transformations

Fibonacci numbers satisfy a wide variety of identities. In order to illustrate the transformation of the identities, we will consider following Fibonacci square type identity [15] :

$$F_{n-1}^2+F_n^2=F_{2n-1}. \tag{31}$$

The ISP of Fibonacci points which are located on the line $y=c_2F_m$ satisfy same type of identity as

follows;

$$2R\left(\frac{\xi^{(3)}_{n-1,m}-R\beta f_{n-1,m}\sin\theta_{n-1,m}\cos\varphi_{n-1,m}}{R(1+\beta f_{n-1,m}\cos\theta_{n-1,m})-\zeta^{(3)}_{n-1,m}}\right)^2 +2R\left(\frac{\xi^{(3)}_{n,m}-R\beta f_{n,m}\sin\theta_{n,m}\cos\varphi_{n,m}}{R(1+\beta f_{n,m}\cos\theta_{n,m})-\zeta^{(3)}_{n,m}}\right)^2 = c_1\frac{\xi^{(3)}_{2n-1,m}-R\beta f_{2n-1,m}\sin\theta_{2n-1,m}\cos\varphi_{2n-1,m}}{R(1+\beta f_{2n-1,m}\cos\theta_{2n-1,m})-\zeta^{(3)}_{2n-1,m}} \tag{32}$$

Similarly, ISP of Fibonacci points which are located on the line $x = c_1F_n$ satisfy same type of identity as follows;

$$2R\left(\frac{\eta^{(3)}_{n,m-1}-R\beta f_{n,m-1}\sin\theta_{n,m-1}\sin\varphi_{n,m-1}}{R(1+\beta f_{n,m-1}\cos\theta_{n,m-1})-\zeta^{(3)}_{n,m-1}}\right)^2 +2R\left(\frac{\eta^{(3)}_{n,m}-R\beta f_{n,m}\sin\theta_{n,m}\sin\varphi_{n,m}}{R(1+\beta f_{n,m}\cos\theta_{n,m})-\zeta^{(3)}_{n,m}}\right)^2 = c_2\frac{\eta^{(3)}_{n,2m-1}-R\beta f_{n,2m-1}\sin\theta_{n,2m-1}\sin\varphi_{n,2m-1}}{R(1+\beta f_{n,2m-1}\cos\theta_{n,2m-1})-\zeta^{(3)}_{n,2m-1}}. \tag{33}$$

Let us consider following Lucas identity [15];

$$L_n^2+L_{n+1}^2=L_{2n}+L_{2n+2} \tag{34}$$

ISP of the special Lucas points $(L_n, 0)$ satisfy following relations; The ξ components of the image points satisfy,

$$\left(\frac{2R^2+2\lambda_nR\sqrt{R^2-(\xi^{(3)}_n-\beta f_nR\sin\theta_n\cos\varphi_n)^2}}{\xi^{(3)}_n-\beta f_nR\sin\theta_n\cos\varphi_n}\right)^2 +\left(\frac{2R^2+2\lambda_{n+1}R\sqrt{R^2-(\xi^{(3)}_{n+1}-\beta f_{n+1}R\sin\theta_{n+1}\cos\varphi_{n+1})^2}}{\xi^{(3)}_{n+1}-\beta f_{n+1}R\sin\theta_{n+1}\cos\varphi_{n+1}}\right)^2 = \frac{2R^2+2\lambda_{2n}R\sqrt{R^2-(\xi^{(3)}_{2n}-\beta f_{2n}R\sin\theta_{2n}\cos\varphi_{2n})^2}}{\xi^{(3)}_{2n}-\beta f_{2n}R\sin\theta_{2n}\cos\varphi_{2n}}+ \frac{2R^2+2\lambda_{2n+2}R\sqrt{R^2-(\xi^{(3)}_{2n+2}-\beta f_{2n+2}R\sin\theta_{2n+2}\cos\varphi_{2n+2})^2}}{\xi^{(3)}_{2n+2}-\beta f_{2n+2}R\sin\theta_{2n+2}\cos\varphi_{2n+2}} \tag{35}$$

and ζ components of the image points satisfy

$$2R\frac{\zeta^{(3)}_n+R(1-\beta f_n\cos\theta_n)}{R(1+\beta f_n\cos\theta_n)-\zeta^{(3)}_n}+2R\frac{\zeta^{(3)}_{n+1}+R(1-\beta f_{n+1}\cos\theta_{n+1})}{R(1+\beta f_{n+1}\cos\theta_{n+1})-\zeta^{(3)}_{n+1}}= \sqrt{\frac{\zeta^{(3)}_{2n}+R(1-\beta f_{2n}\cos\theta_{2n})}{R(1+\beta f_{2n}\cos\theta_{2n})-\zeta^{3}_{2n}}}+\sqrt{\frac{\zeta^{(3)}_{2n+2}+R(1-\beta f_{2n+2}\cos\theta_{2n+2})}{R(1+\beta f_{2n+2}\cos\theta_{2n+2})-\zeta^{(3)}_{2n+2}}} \tag{36}$$

Thus, the identities given in (35) and (36) are the counter part of the identity given in (34) on the deformed spheres. These identities also reduce to the ones on the sphere by choosing $\beta = 0$. In addition to these, the surfaces need not to be differentiable, these identities are also valid for non differentiable surfaces [12]. The other identities satisfied on the deformed spheres for Fibonacci and Lucas points can be found in a similar manner.

4 Inverse Stereographic Projection onto a Deformed Higher Dimensional Sphere

Let $\mathbb{R}^D = \{(X_1, \ldots, X_D)\}$ be the D-dimensional Euclidean space. We consider the $D-1$ dimensional sphere

$$X_1^2+\cdots+X_{D-1}^2+(X_D-R)^2=R^2,\ R>0. \tag{37}$$

The center of this sphere is $C = (0, \ldots, 0, R)$ and its radius is R. Notice that the sphere passes through the origin. We choose the north pole $N = (0, \ldots, 0, 2R)$ as the projection point and the hyperplane $\Pi : X_D = 0$ as the stereographic projection hyperplane. Then, the inverse stereographic projection of $\mathbf{x} = (x_1, \ldots, x_{D-1}, 0) \in \Pi$ onto the sphere is given by

$$X_i=\frac{4R^2x_i}{4R^2+|\mathbf{x}|^2},\qquad i=1,\ldots,D-1, \tag{38}$$

where $|\mathbf{x}|^2 = x_1^2 + \cdots + x_{D-1}^2$, and

$$X_D=\frac{2R|\mathbf{x}|^2}{4R^2+|\mathbf{x}|^2}. \tag{39}$$

Conversely, solving (38)–(39) for the planar coordinates yields the stereographic projection

$$x_i=\frac{2R\,X_i}{2R-X_D},\qquad i=1,\ldots,D-1. \tag{40}$$

Equation (40) will be particularly important in the construction of Fibonacci configurations on the deformed surface.

It is convenient to translate the sphere so that its center coincides with the origin. Define $Y_i = X_i$ for $i = 1, \ldots, D-1$, and $Y_D = X_D - R$. Then (37) becomes $Y_1^2 + \cdots + Y_D^2 = R^2$. Thus, the translated surface is the standard $(D-1)$-dimensional sphere $S_R^{D-1} \subset \mathbb{R}^D$. Consequently, the unit normal vector to the sphere at $\mathbf{Y} \in S_R^{D-1}$ is

$$\mathbf{v}=\frac{\mathbf{Y}}{R}. \tag{41}$$

In component form, $\mathbf{v} = \frac{1}{R}(Y_1, \ldots, Y_D)$. In terms of the original X-coordinates, this becomes

$$\mathbf{v}=\frac{1}{R}\,(X_1,\ldots,X_{D-1},X_D-R). \tag{42}$$

For a sphere, the normal vector is therefore simply the normalized radius vector.

4.1 Normal Deformation of the Sphere

Let $f : S^{D-1} \to \mathbb{R}$ be an arbitrary single-valued function, evaluated at the point $\mathbf{v} = \mathbf{Y}/R$ of the unit sphere, and let β denote the deformation parameter. We deform the sphere in the normal direction according to

$$\mathbf{Y}^d = \mathbf{Y} + \beta R\, f(\mathbf{v})\, \mathbf{v}. \tag{43}$$

Since $\mathbf{v} = \mathbf{Y}/R$, we obtain

$$\mathbf{Y}^d = \big(1 + \beta f(\mathbf{v})\big)\, \mathbf{Y}. \tag{44}$$

Equivalently, the deformation can be written in the form

$$\mathbf{Y}^d = R\left[1 + \beta f(\mathbf{v})\right] \mathbf{v}. \tag{45}$$

Throughout this section we assume

$$1 + \beta f(\mathbf{v}) > 0 \quad \text{for all } \mathbf{v} \in S^{D-1}. \tag{46}$$

For the algebraic relations below, $1 + \beta f(\mathbf{v}) \neq 0$ is sufficient. Condition (46) is needed so that $\mathbf{v}$ can be recovered from the deformed point alone: since $\mathbf{Y}^d = R(1+\beta f)\mathbf{v}$, condition (46) gives $\mathbf{v} = \mathbf{Y}^d/|\mathbf{Y}^d|$, and hence $f(\mathbf{v}) = f\big(\mathbf{Y}^d/|\mathbf{Y}^d|\big)$ depends only on the deformed coordinates. Under (46) the deformed surface is a radial graph over S^{D-1}. No smoothness of f is needed for any of the algebraic relations of this section. We also write $\mathbf{X}^d = \mathbf{Y}^d + R\,\mathbf{e}_D$, with $\mathbf{e}_D = (0, \ldots, 0, 1)$, i.e. $X_j^d = Y_j^d$ for $j = 1, \ldots, D-1$ and $X_D^d = Y_D^d + R$.

4.2 Fibonacci and Lucas Points in $\mathbb{R}^{D-1}$

We now introduce Fibonacci (Lucas) points in the $D-1$ dimensional stereographic hyperplane. Let $\mathbf{n} = (n_1, n_2, \ldots, n_{D-1})$ be a multi-index of non-negative integers and let

$$\mathbf{P}(\mathbf{n}) = \big(\Psi_{n_1}, \Psi_{n_2}, \ldots, \Psi_{n_{D-1}}, 0\big) \tag{47}$$

be a Fibonacci (Lucas) point, where $\Psi_{k+2} = \Psi_{k+1} + \Psi_k$ denotes the classical Fibonacci (Lucas) recurrence. For later convenience, define

$$\rho_{\mathbf{n}}^2 = \sum_{j=1}^{D-1} \Psi_{n_j}^2. \tag{48}$$

Applying the inverse stereographic projection (38)–(39) to $\mathbf{P}(\mathbf{n})$ and translating by $-R\,\mathbf{e}_D$ gives the point $\mathbf{Y}(\mathbf{n})$ on S_R^{D-1} with components

$$Y_j(\mathbf{n}) = \frac{4R^2 \Psi_{n_j}}{4R^2 + \rho_{\mathbf{n}}^2}, \qquad j = 1, \ldots, D-1, \tag{49}$$

and

$$Y_D(\mathbf{n}) = \frac{R\left(\rho_{\mathbf{n}}^2 - 4R^2\right)}{4R^2 + \rho_{\mathbf{n}}^2}. \tag{50}$$

Let $\mathbf{v}_{\mathbf{n}} = \mathbf{Y}(\mathbf{n})/R$ denote the unit normal at the corresponding spherical point, and write

$$f_{\mathbf{n}} := f(\mathbf{v}_{\mathbf{n}}). \tag{51}$$

The deformation factor at this point is

$$\mu_{\mathbf{n}} = 1 + \beta f_{\mathbf{n}}. \tag{52}$$

The deformed Fibonacci point is therefore

$$\mathbf{Y}^d(\mathbf{n}) = \mu_{\mathbf{n}}\, \mathbf{Y}(\mathbf{n}). \tag{53}$$

Since the Fibonacci points are finite, $2R - X_D = R - Y_D > 0$ at every such point, so the north pole is never attained.

4.3 Fibonacci and Lucas Numbers in Terms of the Deformed Surface Coordinates

The inverse stereographic relation (40), expressed in the translated coordinates, is

$$x_j = \frac{2R\, Y_j}{R - Y_D}, \qquad j = 1, \ldots, D-1. \tag{54}$$

Since $Y_j(\mathbf{n}) = Y_j^d(\mathbf{n})/\mu_{\mathbf{n}}$, $Y_D(\mathbf{n}) = Y_D^d(\mathbf{n})/\mu_{\mathbf{n}}$ and $x_j = \Psi_{n_j}$, we obtain

$$\Psi_{n_j} = \frac{2R\left(Y_j^d(\mathbf{n})/\mu_{\mathbf{n}}\right)}{R - Y_D^d(\mathbf{n})/\mu_{\mathbf{n}}}. \tag{55}$$

Multiplying numerator and denominator by $\mu_{\mathbf{n}}$ gives the fundamental relation

$$\Psi_{n_j} = \frac{2R\, Y_j^d(\mathbf{n})}{R\left[1 + \beta f_{\mathbf{n}}\right] - Y_D^d(\mathbf{n})}, \qquad j = 1, \ldots, D-1. \tag{56}$$

Thus, each Fibonacci (Lucas) number can be recovered from a suitable combination of the coordinates of the normally deformed sphere.

Representation in the original X-coordinates. Recall that $Y_j^d = X_j^d$ for $j = 1, \ldots, D-1$, and $Y_D^d = X_D^d - R$. Therefore, equation (56) becomes

$$\Psi_{n_j} = \frac{2R\, X_j^d(\mathbf{n})}{2R + \beta R\, f_{\mathbf{n}} - X_D^d(\mathbf{n})}, \qquad j = 1, \ldots, D-1. \tag{57}$$

Equation (57) is the desired expression of the Fibonacci (Lucas) coordinates in terms of the coordinates of the normally deformed $(D-1)$-sphere. Under (46), $f_{\mathbf{n}} = f\big(\mathbf{Y}^d(\mathbf{n})/|\mathbf{Y}^d(\mathbf{n})|\big)$, so the right-hand side depends only on the deformed coordinates and on f.

An important consistency check is obtained by setting $\beta = 0$. In this case $\mu_{\mathbf{n}} = 1$, and equation (57) reduces to

$$\Psi_{n_j} = \frac{2R\,X_j}{2R - X_D}, \tag{58}$$

which is (40) evaluated at the Fibonacci (Lucas) point. For $D = 3$, the numerator and denominator of (56) are, up to the common factor $\mu_{\mathbf{n}}$, those appearing in relations (29)-(30), the terms $\xi^{(3)} - R\beta f \sin\theta\cos\varphi$ and $R(1 + \beta f\cos\theta) - \zeta^{(3)}$ equal Y_1 and $R - Y_D$, respectively. Relation (56) is the same statement written directly in terms of $\mathbf{Y}^d$.

4.4 Induced Fibonacci and Lucas Recurrence on the Deformed Surface

For a fixed $j \in \{1, \ldots, D-1\}$, $k \in \{0, 1, 2\}$ and a fixed multi-index $\mathbf{n}$, let

$$\mathbf{n}^{(j,k)} = (n_1, \ldots, n_{j-1},\, n_j + k,\, n_{j+1}, \ldots, n_{D-1}), \tag{59}$$

i.e. only the j-th index is shifted while all the other indices are kept fixed. Write $f_{j,k} := f_{\mathbf{n}^{(j,k)}}$, $X_j^d(j,k) := X_j^d(\mathbf{n}^{(j,k)})$ and $X_D^d(j,k) := X_D^d(\mathbf{n}^{(j,k)})$. Note that X_D^d and f depend on n_j also through $\rho_{\mathbf{n}}$, so they change from term to term.

Equation (57) can now be substituted into the Fibonacci (Lucas) recurrence $\Psi_{n_j+2} = \Psi_{n_j+1} + \Psi_{n_j}$. For each fixed coordinate direction j we obtain

$$\begin{aligned}
&\frac{2R\,X_j^d(j,2)}{2R + \beta R f_{j,2} - X_D^d(j,2)} \\
&= \frac{2R\,X_j^d(j,1)}{2R + \beta R f_{j,1} - X_D^d(j,1)} \\
&+ \frac{2R\,X_j^d(j,0)}{2R + \beta R f_{j,0} - X_D^d(j,0)},
\end{aligned} \tag{60}$$

where $f_{j,k} = f\big(\mathbf{v}_{\mathbf{n}^{(j,k)}}\big)$. It must be noted that Equation (60) is a compact form of $D-1$ relations ($j = 1, \ldots, D-1$), and shows that the Fibonacci recurrence can be expressed entirely through suitable combinations of the coordinates of the deformed surface together with the deformation function. In this way, a new form of the Fibonacci numbers in terms of the deformation function and the deformation parameter, which describe the geometry of the surface, has been obtained.

5 Conclusion

In the present work, inverse stereographic projection of the Fibonacci and Lucas points on to the deformed spheres are considered. Deformed spheres are obtained by the deformation of spheres with single valued deformation functions. It was shown that image of the Fibonacci and Lucas points are not completely arbitrary but satisfy recurrence relations. More interestingly, those relations contain surface deformation functions thus they depend on the shape and size of the deformed spheres. Since deformations of sphere are arbitrary, the present obtained results are valid for infinitely many different surfaces. According to the deformation functions, these surfaces could be rotationally symmetric or non-symmetric, differentiable or non- differentiable. Thus present work construct a new path between abstract number theory and surface theory.

Acknowledgment: The author would like to express sincere gratitude to the Editor for kindly agreeing to publish this article free of charge, and for supporting scientific research and the open dissemination of knowledge. The author is also grateful to the three anonymous reviewers for their careful reading of the manuscript and for their valuable comments and constructive suggestions, which improved the quality of the paper.

Declaration of Generative AI and AI-assisted Technologies in the Writing Process

During the preparation of this work, the author(s) utilized artificial intelligence (AI) technologies solely for the purpose of linguistic refinement and grammatical correction. Following the application of these tools, the author(s) comprehensively reviewed, verified, and edited the resulting text. The author(s) maintain full accountability and responsibility for the accuracy, integrity, and final content of the publication.

References:

[1] Cruz N., Olivares M., Villanueva J., The golden ratio in Schwarzschild-Kottler black holes, The European Physical Journal C, Vol. 77, No. 2, 2017, pp. 1-6.

[2] Pletser V., Fibonacci numbers and the golden ratio in biology, physics, astrophysics, chemistry and technology: A non-exhaustive review, arXiv preprint, 2017, arXiv:1801.01369.

[3] Segerman H., et al., The sunflower spiral and the Fibonacci metric,Proceedings of Bridges, Vol. 20, No. 10, 2010, pp. 483-486.

[4] Hayashi M., Katsu A., Ogiso Y., Takaki, R., Simulations of sunflower spirals and Fibonacci numbers,Forma-Tokyo, Vol. 18, No. 4, 2003, pp. 295-305.

[5] Akhtaruzzaman M., Shafie A. A., Geometrical substantiation of Phi, the golden ratio and the baroque of nature, architecture, design and engineering, International Journal of Arts, Vol. 1, No. 1, 2011, pp. 1-22.

[6] Kustepeli A., Ozbakis B., The resonant behavior of the Fibonacci fractal tree antennas,Microwave and Optical Technology Letters, Vol. 50, No. 4, 2008, pp. 1046-1050.

[7] Bohnet J.G., Dumitrescu, P.T., Gaebler, J.P. et al., Dynamical topological phase realized in a trapped ion quantum simulator, Nature, Vol. 607, 2022, pp. 63467.

[8] Ahlfors L. V., Complex analysis: An introduction to the theory of analytic functions of one complex variable,McGraw-Hill,1953. ISBN M7-000657-1

[9] Silverman R. A., Complex analysis with applications,Courier Corporation, 1984. ISBN: 9780486647623

[10] B. Ates, S.Ates, A.Kustepeli, A Novel Approach to the Fibonacci Numbers by Inverse Stereographic Projection,TWMS J. App. and Eng. Math, Vol. 16, No. 8, 2026, pp. 938–952.

[11] B. Ates, S. Ates and A. Kustepeli, "Fibonacci Points and Inverse Stereographic Projection",2nd Kocaeli Science Congress (KOSC-2025) Book of Proceedings, 2025, [Online]. https://zenodo.org/records/18011963 (Accessed Date: January 30, 2026).

[12] B. Ates, A. Kustepeli, Generalization of Stereographic Projection,Hal Science, hal-05098845, 2025, [Online]. https://hal.science/hal-05098845 (Accessed Date: January 30, 2026).

[13] Karlığa, Baki, On The Generalized Stereographic Projection,Contributions To Algebra and Geometry, Vol. 37, No. 2, 1996, pp. 329-336.

[14] B. Ates, "Inverse Stereographic Projection of Fibonacci Points onto the Quadric Surfaces",Communications in Advanced Mathematical Sciences, Vol. 9, No. 1, 2026, pp. 34–49.

[15] Koshy T., Fibonacci and Lucas numbers with applications, John Wiley & Sons, 2001, ISBN: 9780471399698, DOI: 10.1002/9781118033067.

Contribution of Individual Authors to the Creation of a Scientific Article (Ghostwriting Policy)

The author contributed in the present research, at all stages from the formulation of the problem to the final findings and solution.

Sources of Funding for Research Presented in a Scientific Article or Scientific Article Itself

No funding was received for conducting this study.

Conflict of Interest

The author has no conflict of interest to declare that is relevant to the content of this article.

Creative Commons Attribution License 4.0 (Attribution 4.0 International, CC BY 4.0)

This article is published under the terms of the Creative Commons Attribution License 4.0
https://creativecommons.org/licenses/by/4.0/deed.en_US